structural communications

Acta Crystallographica Section F
Structural Biology Communications

ISSN 2053-230X

Structure of an *Aspergillus fumigatus* old yellow enzyme (EasA) involved in ergot alkaloid biosynthesis

Annemarie S. Chilton, Ashley L. Ellis and Audrey L. Lamb*

Molecular Biosciences, University of Kansas, 1200 Sunnyside Avenue, Lawrence, KS 66045, USA

Correspondence e-mail: lamb@ku.edu

Received 22 July 2014
Accepted 21 August 2014

PDB reference: EasA, 4qnw

The *Aspergillus fumigatus* old yellow enzyme (OYE) EasA reduces chanoclavine-I aldehyde to dihydrochanoclavine aldehyde and works in conjunction with festuclavine synthase at the branchpoint for ergot alkaloid pathways. The crystal structure of the FMN-loaded EasA was determined to 1.8 Å resolution. The active-site amino acids of OYE are conserved, supporting a similar mechanism for reduction of the α/β-unsaturated aldehyde. The C-terminal tail of one monomer packs into the active site of a monomer in the next asymmetric unit, which is most likely to be a crystallization artifact and not a mechanism of self-regulation.

1. Introduction

Ergot alkaloids are produced by fungi and plants and have historically been used medicinally and for psychedelic recreation (lysergic acid derivatives), and have been the cause of poisonings with symptoms that were attributed to witchcraft (Schardl *et al.*, 2006). These secondary metabolites are derived from tryptophan and dimethylallyl diphosphate (DMAPP) and are characterized by the tetracyclic ergoline ring system, of which festuclavine is one of the simplest examples, or characterized by the tricyclic ring system exemplified by chanoclavine-I aldehyde (Fig. 1*a*; Schardl *et al.*, 2006). Isotope-feeding studies suggest that chanoclavine-I aldehyde may be a common intermediate for the biosynthesis of all ergot alkaloids (Floss *et al.*, 1974). Conversion of chanoclavine-I aldehyde to dihydrochanoclavine aldehyde by *Aspergillus fumigatus* has been reported to require an old yellow enzyme (OYE) called EasA (Cheng *et al.*, 2010*a*,*b*; Coyle *et al.*, 2010; Geu-Flores *et al.*, 2012) or FgaOx3 (Wallwey *et al.*, 2010) for the reduction of the α/β-unsaturated aldehyde. The dihydrochanoclavine aldehyde is subsequently cyclized to form an iminium compound. It is unknown whether the cyclization is enzyme-catalyzed. A second reduction step to produce festuclavine from the iminium compound is performed by the NADH-dependent festuclavine synthase FgaFS (Wallwey *et al.*, 2010).

The *Saccharomyces pastorianus* old yellow enzyme was the first flavoenzyme to be identified (Warburg & Christian, 1932). Members of the OYE family are found in bacteria, fungi and plants, and catalyze the reduction of activated carbon–carbon double bonds (for excellent reviews, see Stuermer *et al.*, 2007; Williams & Bruce, 2002). Here, we present the structural characterization of the *A. fumigatus* OYE EasA involved in ergot alkaloid biosynthesis. These data allow us to corroborate the proposed mechanism and to provide insight into the oligomerization of EasA in solution and in the crystal.

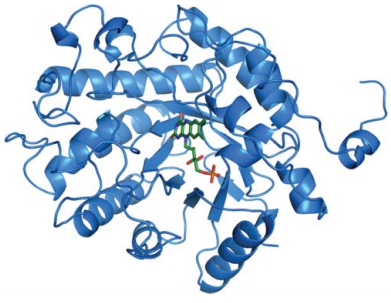

2. Materials and methods

2.1. Macromolecule production

The preparation of the expression vector has been described previously (Cheng *et al.*, 2010*a*). The expression vector, which generates C-terminally histidine-tagged EasA, was transformed into *Escherichia coli* BL21(DE3) cells, which were grown in LB broth containing 50 µg ml^{-1} kanamycin at 37°C with shaking (175 rev min^{-1}) for 2.5 h. The temperature was reduced to 15°C for 1 h until an optical density at 600 nm of ∼0.1 was reached. Protein expression was induced with 50 µ*M* IPTG and the cultures were

incubated for 64 h. Cells were harvested by centrifugation (3800*g*, 4°C, 10 min). The cell pellet was resuspended in 10 ml 5 m*M* imidazole, 300 m*M* NaCl, 20 m*M* Tris–HCl pH 8.0, 10% glycerol (buffer *A*). The cells were disrupted using a French pressure cell (241 MPa) and cellular debris was removed by centrifugation (20 800*g*, 4°C, 1 h). The lysate was applied onto 50 ml Ni–NTA resin (Qiagen) in a Kontes column equilibrated with buffer *A*. The column was shaken to mix the lysate with the resin and incubated overnight at 4°C on a gently tilting base. After 21 h, EasA was eluted from the Ni–NTA column with a step gradient of imidazole (5, 25, 50, 100, 150 and 300 m*M*) in buffer *A*. EasA primarily eluted at 150 m*M* imidazole.

To load the EasA protein with FMN (flavin mononucleotide), a previously published procedure (Gatti *et al.*, 1994) was modified. A Red Sepharose (GE Healthcare) column was pre-equilibrated with three column volumes of buffer *B* (50 m*M* potassium phosphate monobasic pH 7.0, 10% glycerol). The 150 m*M* imidazole Ni–NTA fractions (~50 ml) were concentrated to 25 ml and diluted in buffer *B* to a final estimated salt concentration of ~25 m*M* NaCl. The sample was injected and washed with eight column volumes of buffer *B* followed by a linear gradient of 0–600 m*M* NaCl (five column volumes) in buffer *B* to wash out unbound sample. The column was washed with two column volumes of buffer *B* with 10 µ*M* FMN. EasA was eluted using a 20-column-volume linear gradient from 0 to 2 *M* NaCl with 10 µ*M* FMN in buffer *B*.

The fractions containing EasA from the Red Sepharose column were pooled and applied onto a Superdex 200 size-exclusion column (GE Healthcare) pre-equilibrated with 50 m*M* Tris–HCl, 150 m*M* sodium citrate, 10% glycerol pH 8.0. The fractions containing EasA were pooled, concentrated to 3 mg ml^{-1} using an Amicon stirred cell with a YM-30 membrane and stored at −80°C. Approximately 9 mg EasA was purified from 4 l culture. EasA eluted from the size-exclusion column was ~85% FMN-bound. The amount of FMN loading was determined by comparing the concentration of EasA, determined by measuring the A_{280} (in deionized water ε = 56 840 M^{-1} cm^{-1}), and the concentration of FMN, determined by measuring the A_{446} (ε = 11 500 M^{-1} cm^{-1}).

2.2. Crystallization

Crystals were grown at 25°C using the hanging-drop vapor-diffusion method with 750 µl reservoir solution consisting of 230 m*M* ammonium sulfate, 100 m*M* MES pH 6.0, 30% PEG 8000. The hanging drops consisted of 1.5 µl reservoir solution and 1.5 µl 24 mg ml^{-1} protein. Yellow crystals were fully developed in 4 d with approximate dimensions of 160 × 40 × 20 µm. For data collection, crystals were transferred to the reservoir solution supplemented with 20% glycerol solution and were flash-cooled by plunging them into liquid nitrogen.

2.3. Data collection and processing

X-ray diffraction data were collected on beamline 11-1 at the Stanford Synchrotron Radiation Laboratory (SSRL), Stanford,

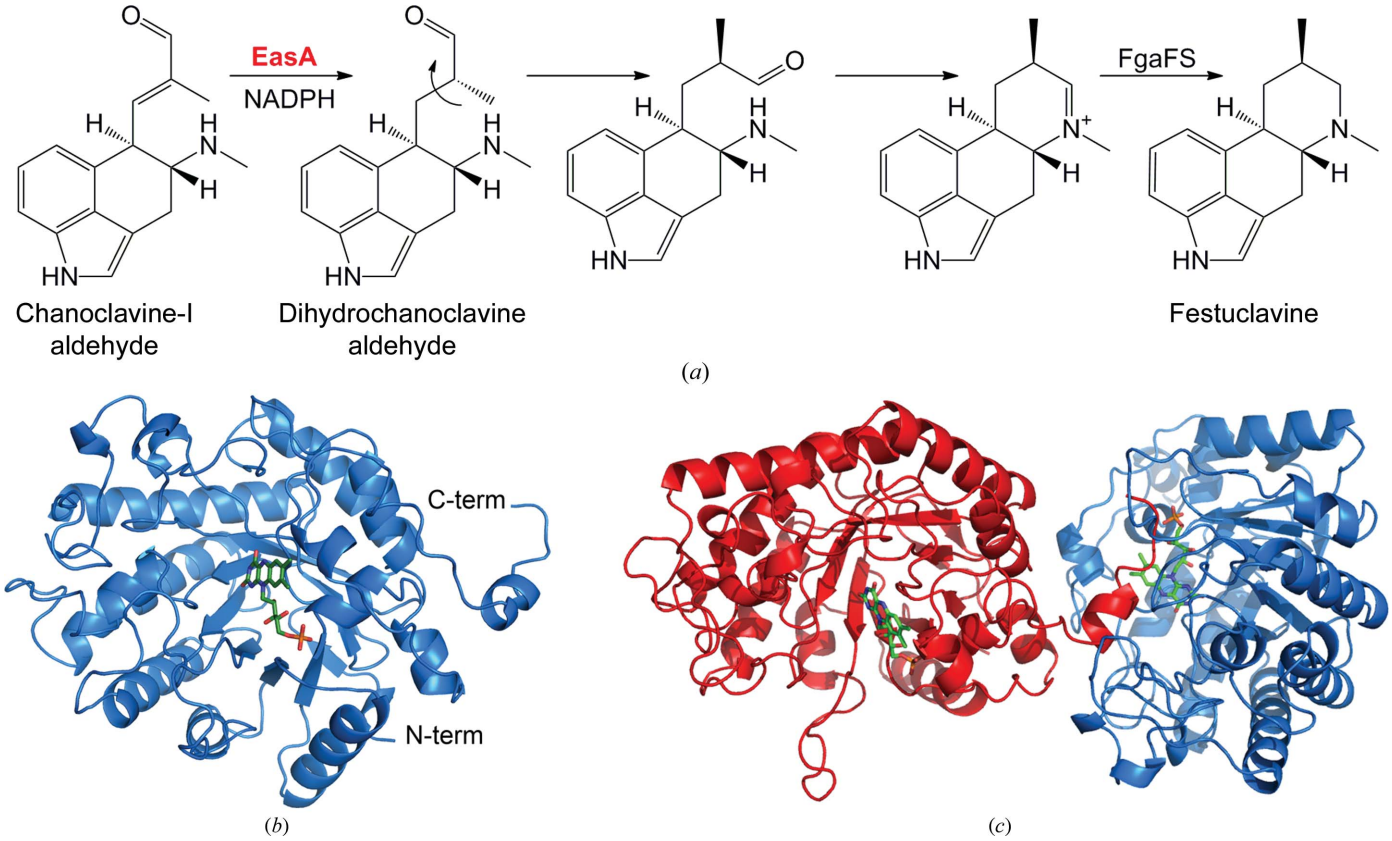

Figure 1
EasA mechanism and overall structure. (*a*) The reaction catalyzed by the old yellow enzyme EasA from *A. fumigatus*, the conversion of chanoclavine-I aldehyde to dihydrochanoclavine, is labeled in red. The next two reactions are hypothesized to be spontaneous. The final reaction for the generation of festuclavine is catalyzed by FgaFS, festuclavine synthase. (*b*) EasA is a classic α/β-barrel, shown as a blue cartoon. The FMN (green sticks) is bound in the active-site funnel composed by eight parallel strands of the β-barrel. The backside of the barrel is closed by a two-stranded β-sheet: the two strands that precede the first strand of the barrel at the N-terminus of the protein. (*c*) The C-terminal tail of the red monomer packs in the active site of the blue monomer in the next asymmetric unit. The location of the active site is noted by the inclusion of the FMN as green sticks. Protein structure pictures were generated in *PyMOL* (Schrödinger).

Table 1
Data collection and processing.

Values in parentheses are for the outer shell.

Diffraction source	SSRL beamline 11-1
Wavelength (Å)	0.97945
Temperature (°C)	−173
Detector	PILATUS 6M
Crystal-to-detector distance (mm)	260
Rotation range per image (°)	0.5
Total rotation range (°)	180
Exposure time per image (s)	20
Space group	$P2_12_12_1$
a, b, c (Å)	62.5, 65.9, 115.2
α, β, γ (°)	90, 90, 90
Resolution range (Å)	38.41–1.80 (1.90–1.80)
Total No. of reflections	162475 (23165)
No. of unique reflections	44595 (6332)
Completeness (%)	99.3 (97.6)
Multiplicity	3.6 (3.7)
$\langle I/\sigma(I)\rangle$	23.6 (3.3)
$R_{\rm merge}$	0.040 (0.399)

Table 2
Structure refinement.

Values in parentheses are for the outer shell.

Resolution range (Å)	35.630–1.799 (1.846–1.799)
No. of reflections	40082 (2851)
Final $R_{\rm cryst}$	0.178 (0.221)
Final $R_{\rm free}$	0.221 (0.273)
Total unique observations	40082
No. of non-H atoms	
Protein	2916
Solvent (sulfate and glycerol)	26
FMN	31
Water	239
R.m.s. deviations	
Bonds (Å)	0.026
Angles (°)	2.02
Overall mean B factor (Å^2)	21.6

Califonia, USA using a wavelength of 0.97945 Å. Data (180°) were collected as 0.5° oscillation images (20 s exposure per frame) using *Blu-Ice* (Soltis *et al.*, 2008) with a crystal-to-detector distance of 260 mm at −173°C. The crystals were assigned to space group $P2_12_12_1$, with unit-cell parameters $a = 62.5$, $b = 65.9$, $c = 115.2$ Å. The data were indexed and scaled to 1.80 Å resolution using the *XDS* program package (Kabsch, 2010).

2.4. Structure solution and refinement

Molecular-replacement calculations were performed using *Phaser* (McCoy *et al.*, 2007) with data from 38.36 to 2.5 Å resolution. A structure of old yellow enzyme (PDB entry 1oya; Fox & Karplus, 1994) was used as a search model with FMN and waters removed, yielding a clear solution with a log-likelihood gain of greater than 400. The packing criterion in the automated search had to be changed to allow a maximum number of clashes of 20 with a clash distance of 3.0 for a solution to be generated. This is not surprising in light of the packing, which will be discussed later. The map generated with this solution showed unmodeled electron density in the active site corresponding to FMN and additional residues at the C-terminus. These differences in electron density relative to the molecular-replacement model indicate a correct solution. The FMN was built into the density and the C-terminal tail was added followed by iterative rounds of model building and refinement using *Coot* (Emsley & Cowtan, 2004) and *REFMAC*5 (Murshudov *et al.*, 2011). Waters were added using the water-addition function in *Coot*, and the suggested positions were manually verified in *Coot* following a refinement cycle in *REFMAC*5. The model was validated using *MolProbity* (Chen *et al.*, 2010). Areas of geometric outliers are concentrated in the loops containing residues 121–123 and residues 134–138, which had poor electron density likely owing to disorder, including the single Ramachandran outlier, which was found at residue 136. Data-collection and refinement statistics can be found in Tables 1 and 2. The coordinates and structure factors have been deposited in the Protein Data Bank with accession code 4qnw.

3. Results and discussion

3.1. Purification of EasA and loading with FMN

The preparation of EasA using a heterologous expression system has previously been reported to typically produce enzyme that was 20–25% loaded with the FMN cofactor (Cheng *et al.*, 2010*a*). In our hands, we generally produced protein that had an even lower percentage of FMN bound (0–6%) by a comparable purification strategy using nickel-affinity chromatography (the protein is histidine-tagged). However, a purification step was added in which Red Sepharose is used to bind EasA (owing to its affinity for the flavin) and the protein is eluted from the column using sodium chloride in the presence of FMN. This is an adaptation of the protocol used to exchange the natural flavin in *p*-hydroxybenzoate hydroxylase for 6-azido FAD (Gatti *et al.*, 1994). Finally, the protein was subjected to size-exclusion chromatography, where it eluted as a monomer. This complete purification procedure produced approximately 2.25 mg of ∼85% FMN-loaded EasA per litre of *E. coli* culture. The purified protein includes a ten-amino-acid linker followed by a six-residue histidine tag at the C-terminus.

3.2. Overall structure of EasA

The structure of EasA was determined by molecular replacement using *S. pastorianus* OYE (PDB entry 1oya; Fox & Karplus, 1994), which has 39.5% sequence identity as calculated by *LALIGN* (Huang & Miller, 1991), as the search model. The final model includes a single monomer containing residues 8–376 without chain breaks: the first seven amino acids and the C-terminal linker and histidine tag are not visible in the model. There is poor density for the loops containing residues 121–123 and residues 134–138, causing poor geometric values in these areas. A molecule of FMN is found in the active site. There are also four sulfate ions and one glycerol molecule derived from the mother liquor and the cryoprotectant. The model is completed with 239 water molecules.

Not surprisingly, EasA is a strong structural homolog of OYE (r.m.s.d. of 1.15 Å for 331 C$^\alpha$ atoms). The structure is a classic α/β-barrel built up by consecutive α/β motifs to form a central eight-stranded parallel β-barrel surrounded by α-helices (Fig. 1*b*). The N-terminus forms a short antiparallel two-stranded β-sheet that closes off the back of the barrel. The FMN is bound at the other end of the barrel, in an analogous position to the FMN in OYE. Strong density can be seen in the simulated-annealing composite OMIT map with the occupancy set to 1.0, suggesting that the crystallized protein is fully loaded with FMN (Fig. 2*a*). The *B* factors for the FMN (ranging from 13 to 24 Å^2) are in good agreement with those of the surrounding amino-acid side chains, providing quantitative evidence for full occupancy. The FMN was initially modeled using the oxidized configuration, but is not strictly planar in the final model; however, the FMN is not well modeled by the butterfly bend of a reduced flavin. It is likely that a fraction of the flavin molecules in the crystal were reduced by the X-rays during the diffraction experiment and this model represents the average of the oxidized and reduced states found in the crystal.

The catalytic residues found in OYE are conserved in EasA, as was predicted from sequence alignments (Cheng *et al.*, 2010*a*). A mechanism for the reduction of chanoclavine-I aldehyde to dihydrochanoclavine aldehyde has been proposed (Cheng *et al.*, 2010*a*) based on the extensive literature for old yellow enzymes (Brown *et al.*, 1998, 2002; Fox & Karplus, 1994; Karplus *et al.*, 1995; Kohli & Massey, 1998; Meah *et al.*, 2001; Williams & Bruce, 2002; Xu *et al.*, 1999). In this mechanism, the reductive half reaction allows reduction of the FMN by NADPH. In the oxidative half reaction, His173 or Asn176 hydrogen bond to the substrate aldehyde. A hydride is transferred from the reduced FMN to the β-carbon of the aldehyde, while Tyr178 serves as a proton donor to the α-carbon. The hydride and proton transfers may be concurrent or sequential (Cheng *et al.*, 2010*a*; Kohli & Massey, 1998). The amino acids of the proposed mechanism are indeed structurally conserved (Fig. 2*b*) and the structure determined here is consistent with this mechanism.

3.3. Protein oligomerization

A monomer of one asymmetric unit packs with the C-terminus in the active site of the monomer in the next asymmetric unit, forming a fiber (Fig. 1*c*). Residues 371–376 of one monomer are adjacent to the FMN (Fig. 2*c*); however, none of the residues of the linker or histidine tag that follow the natural C-terminus are visible in the electron-density maps, and would have exited the opposite side of the active-site cleft. Many attempts were made to produce crystals with different packing interactions and in different crystal morphologies. These included crystallizing with NADPH, $NADP^+$, substrate or substrate analogs to block binding of the C-terminus in the active site. The N-terminally His-tagged protein did not crystallize. Deletion constructs of various lengths at the C-terminus (both in the N- and C-terminally tagged clones) could not be overproduced in *E. coli*. EasA without a histidine tag could not be overproduced.

There is evidence for self-regulation in this structural class of enzymes by packing of a loop into the active site. The OYE homolog 12-oxophytodienoate reductase 3 (OPR3) crystallizes with loop 6 inserted into the active site of the opposing monomer, making an inactivated homodimer (Breithaupt *et al.*, 2006). OPR3 was likewise shown by size-exclusion chromatography, dynamic light scattering and analytical ultracentrifugation to exist in a monomer–dimer equilibrium in solution and was proposed to be regulated by homodimerization upon a phosphorylation event that was mimicked

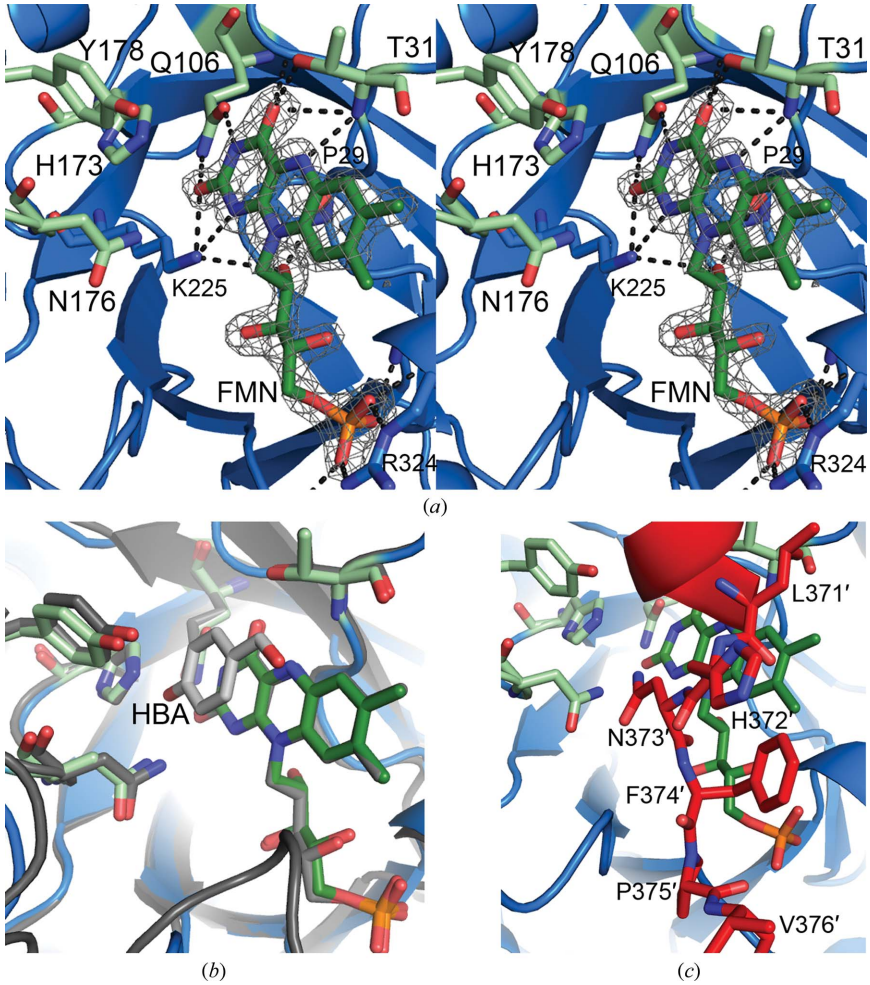

Figure 2
EasA active site. (*a*) The EasA active site is shown in stereo as a blue cartoon with the active-site residues hypothesized previously shown as light green sticks. By comparison to OYE, these residues were proposed to be involved in FMN binding (Thr31 and Gln106), NADPH binding (His173 and Asn176) and reduction of the substrate (His173, Asn176 and Tyr178) (Cheng *et al.*, 2010*a*). The residues shown as blue sticks (Pro29, Lys225 and Arg324) hydrogen bond (dashed lines) to the FMN. The FMN is shown as dark green sticks surrounded by a $2F_o - F_c$ simulated-annealing composite OMIT electron-density map (grey cages) contoured at 1.5σ. The composite OMIT map was generated using *PHENIX* (Adams *et al.*, 2010). (*b*) Overlay of EasA with old yellow enzyme with *p*-hydroxybenzaldehyde (HBA) bound (PDB entry 1oyb; Fox & Karplus, 1994), highlighting the location where chanoclavine-I aldehyde would bind. EasA is colored as in (*a*) and OYE is colored grey. (*c*) The extreme C-terminus of the monomer from the adjacent unit cell, residues 371′–376′ (shown in red), packs in the active site adjacent to the FMN, blocking access of substrate or NADPH.

in the crystallization by a solvent-derived sulfate (Breithaupt *et al.*, 2006).

Most likely, the oligomerization observed in the EasA crystals is a crystal-packing artifact. The amino acids that pack into the active site are not derived from the same segment of polypeptide (an internal loop in OPR3 *versus* the C-terminal tail in EasA). The C-terminal tail of EasA is long enough to pack in the active site of the same monomer (monomeric self-regulation), but only with a considerable conformational change. The simplest rearrangement would orient the C-terminus in the wrong direction relative to the observed binding. A dimerization based on this interaction with the C-termini in the opposing active sites would also be feasible (dimeric self-regulation): there is sufficient length but a considerable conformational change would be required. Self-regulation by packing of the C-terminus into the active site (either monomeric or dimeric self-regulation) cannot be ruled out, but there is no corroborating evidence. Size-exclusion chromatography indicates that the protein is monomeric even at high concentration, and previous kinetic observations showed standard Michaelis–Menten kinetics (Cheng *et al.*, 2010*a*).

We are grateful to several people for ideas and assistance. This project was initiated at the suggestion of Sarah E. O'Connor. The plasmids were a gift from her laboratory and the expression protocols were established with the help of Johnathan Z. Cheng. Graham R. Moran suggested the use of Red Sepharose to load the protein with FMN. Andrew N. Ouellette, Jose Olucha and Kathleen M. Meneely aided with crystal mounting, data collection and model refinement. Diffraction data were collected at the Stanford Synchrotron Radiation Laboratory, a national user facility operated by Stanford University on behalf of the US Department of Energy, Office of Basic Energy Sciences. The SSRL Structural Molecular Biology Program is supported by the Department of Energy, Office of Biological and Environmental Research and by the National Institutes of Health, National Center for Research Resources, Biomedical Technology Program and the National Institute of General Medical Sciences. We would like to thank the staff at the Stanford Synchrotron Radiation Laboratory for their support and assistance. This publication was made possible by funds from the grant K02 AI093675 from the National Institute for Allergy and Infectious Disease (ALL) and by a Kansas-IDeA Network for Biomedical Excellence Undergraduate Scholarship (ALE) supported by grants P20 RR016475 from the National Center for Research Resources and P20GM103418 from the National Institute of General Medical Sciences, all from the National Institutes of Health.

References

Adams, P. D. *et al.* (2010). *Acta Cryst.* D**66**, 213–221.
Breithaupt, C., Kurzbauer, R., Lilie, H., Schaller, A., Strassner, J., Huber, R., Macheroux, P. & Clausen, T. (2006). *Proc. Natl Acad. Sci. USA*, **103**, 14337–14342.
Brown, B. J., Deng, Z., Karplus, P. A. & Massey, V. (1998). *J. Biol. Chem.* **273**, 32753–32762.
Brown, B. J., Hyun, J.-W., Duvvuri, S., Karplus, P. A. & Massey, V. (2002). *J. Biol. Chem.* **277**, 2138–2145.
Chen, V. B., Arendall, W. B., Headd, J. J., Keedy, D. A., Immormino, R. M., Kapral, G. J., Murray, L. W., Richardson, J. S. & Richardson, D. C. (2010). *Acta Cryst.* D**66**, 12–21.
Cheng, J. Z., Coyle, C. M., Panaccione, D. G. & O'Connor, S. E. (2010*a*). *J. Am. Chem. Soc.* **132**, 1776–1777.
Cheng, J. Z., Coyle, C. M., Panaccione, D. G. & O'Connor, S. E. (2010*b*). *J. Am. Chem. Soc.* **132**, 12835–12837.
Coyle, C. M., Cheng, J. Z., O'Connor, S. E. & Panaccione, D. G. (2010). *Appl. Environ. Microbiol.* **76**, 3898–3903.
Emsley, P. & Cowtan, K. (2004). *Acta Cryst.* D**60**, 2126–2132.
Floss, H. G., Tcheng-Lin, M., Chang, C.-J., Naidoo, B., Blair, G. E., Abou-Chaar, I. & Cassady, J. M. (1974). *J. Am. Chem. Soc.* **96**, 1898–1909.
Fox, K. M. & Karplus, P. A. (1994). *Structure*, **2**, 1089–1105.
Gatti, D. L., Palfey, B. A., Lah, M. S., Entsch, B., Massey, V., Ballou, D. P. & Ludwig, M. L. (1994). *Science*, **266**, 110–114.
Geu-Flores, F., Sherden, N. H., Courdavault, V., Burlat, V., Glenn, W. S., Wu, C., Nims, E., Cui, Y. & O'Connor, S. E. (2012). *Nature (London)*, **492**, 138–142.
Huang, X. & Miller, W. (1991). *Adv. Appl. Math.* **12**, 337–357.
Kabsch, W. (2010). *Acta Cryst.* D**66**, 125–132.
Karplus, P. A., Fox, K. M. & Massey, V. (1995). *FASEB J.* **9**, 1518–1526.
Kohli, R. M. & Massey, V. (1998). *J. Biol. Chem.* **273**, 32763–32770.
McCoy, A. J., Grosse-Kunstleve, R. W., Adams, P. D., Winn, M. D., Storoni, L. C. & Read, R. J. (2007). *J. Appl. Cryst.* **40**, 658–674.
Meah, Y., Brown, B. J., Chakraborty, S. & Massey, V. (2001). *Proc. Natl Acad. Sci. USA*, **98**, 8560–8565.
Murshudov, G. N., Skubák, P., Lebedev, A. A., Pannu, N. S., Steiner, R. A., Nicholls, R. A., Winn, M. D., Long, F. & Vagin, A. A. (2011). *Acta Cryst.* D**67**, 355–367.
Schardl, C. L., Panaccione, D. G. & Tudzynski, P. (2006). *Alkaloids Chem. Biol.* **63**, 45–86.
Soltis, S. M. *et al.* (2008). *Acta Cryst.* D**64**, 1210–1221.
Stuermer, R., Hauer, B., Hall, M. & Faber, K. (2007). *Curr. Opin. Chem. Biol.* **11**, 203–213.
Wallwey, C., Matuschek, M., Xie, X.-L. & Li, S.-M. (2010). *Org. Biomol. Chem.* **8**, 3500–3508.
Warburg, O. & Christian, W. (1932). *Naturwissenschaften*, **20**, 688.
Williams, R. E. & Bruce, N. C. (2002). *Microbiology*, **148**, 1607–1614.
Xu, D., Kohli, R. M. & Massey, V. (1999). *Proc. Natl Acad. Sci. USA*, **96**, 3556–3561.